Hindawi
Structural Control and Health Monitoring
Volume 2023, Article ID 2558070, 18 pages
https://doi.org/10.1155/2023/2558070

Research Article

Design of Optimal Passive Tuned Mass Damper with Static Output Feedback and Updating Iterative Procedure

Yong-An Lai[1], **Chi-Hung Chang**[1], **Cho-Yen Yang**[2] and **Chia-Ming Chang**[3]

[1]*Department of Civil Engineering, National Central University, Taoyuan 320317, Taiwan*
[2]*National Center for Research on Earthquake Engineering, Taipei 106219, Taiwan*
[3]*Department of Civil Engineering, National Taiwan University, Taipei 106319, Taiwan*

Correspondence should be addressed to Yong-An Lai; laiyongan@ncu.edu.tw

Received 1 December 2022; Revised 12 May 2023; Accepted 16 May 2023; Published 3 June 2023

Academic Editor: Sara Casciati

In this study, the optimal design issue of a passive tuned mass damper (TMD) was transformed into the nonsparse control gain matrix optimization problem, and a general passive TMD optimization design method to minimize structural mean square responses or impulse response is therefore proposed. The proposed optimization procedure combines the static output feedback (also known as direct output feedback) algorithm and the updating iterative procedure. The proposed method can be applied to variant design scenario, whether the main structure is single-degree-of-freedom (SDOF) or multidegree-of-freedom (MDOF) structures, undamped or damped structures, subjected to wind disturbances or earthquake excitations. In addition, the proposed method is capable to consider the excitation shaping filter, so the design results are more suitable for practical application. The design procedure of the proposed method is presented, and all the required weighting matrices are introduced and derived in detail. Firstly, the SDOF structures are used as the main structure to demonstrate the correctness of the proposed method. The numerical simulation results verify that the obtained optimal design parameters of TMD were found identical to some cases which contain the analytic solution. The accuracy and feasibility of the proposed design method are confirmed. Finally, a passive TMD is optimally designed for a 5-story MDOF structure subjected to Kanai–Tajimi spectrum comparable earthquakes and a 60-story high-rise MDOF structure subjected to Davenport spectrum comparable wind loads for demonstration.

1. Introduction

Building structures are often subjected to external forces such as wind loads or earthquakes. In order to improve the resilience capability of building structures, the application of passive damping systems to reduce the vibration response of the structure is a feasible approach. Soong and Dargush [1] and Li [2] introduced various types of linear and nonlinear passive damping systems and their applications to reduce structural vibrations. Recently, Takewaki and Akehashi [3] further reviewed the application of passive damping systems for nonlinear structures from 1980s. Among the many passive energy dissipation systems, TMD is one common passive damping device that can effectively reduce the structural response. Unlike other types of passive energy dissipation devices that are distributed across many floors of buildings, the TMD is usually installed at the top of buildings. Therefore, the TMD is effective in reducing the structural response of the specific tuning mode, whether other floor-distributed installed dampers are effective for more natural modes of the MDOF building structure [4].

The tuned mass damper or dynamic vibration absorber (DVA) is a passive structural vibration control device, as a substructure system assembled by mass, damping, and stiffness. The substructure system employed on the main structure can change its dynamic characteristics. When the natural frequency of the substructure is close to the vibration frequency of the main structure, the vibration energy of the main structure is transferred to the substructure system according to the resonance effect. This reduces the vibration energy of the main structure, thereby decreasing the dynamic response and enhancing the safety and comfort of the

main structure. Since Frahm [5] proposed a patent that incorporates a mass-spring system into a structure as a damping device, the passive TMD has attracted the attention of civil and mechanical engineers worldwide. At present, the passive TMD has been successfully used in many tall buildings, such as the two sets of 360-ton TMDs that are diagonally installed on the 58th floor of the John Hancock building in Boston (height 244 m) [6] and one set of 660-ton suspension TMD that is installed on the 92nd floor of the Taipei 101 building in Taipei (height 508 m) [7]. For the buildings installed with TMD, the wind-induced acceleration was reduced by about 40% in record [1]. For existing structures, the fundamental natural frequency of the building structures is often gradually decreased during their life cycle. Therefore, re-evaluating and retrofitting the design parameters of the TMD to maintain its vibration reduction effect have also been a significant issue in recent years [8, 9].

The optimal design of TMD is a topic that attracts the interest of engineers. Den Hartog [10] incorporated the TMD into the undamped SDOF structure subjected to external harmonic disturbance and used the "fix-point" in the frequency response function to deduce a set of optimal design formulae. Tsai and Lin [11] proposed an optimal design formula for the undamped SDOF structure in the harmonic base excitation in the concept of fix-point theory and further obtained the design formula for the damped structure by regression. Warburton [12] proposed the optimization formula to minimize the mean square response of structural displacement or velocity for undamped structures subjected to random wind load or earthquake load. Furthermore, the optimization formula of analytic solutions or approximate solutions for various cases of objective and disturbance was compiled and proposed by Korenev and Reznikov [13]. Later, Bakre and Jangid [14] obtained the optimal design formula by regression for mean square response minimization of structural displacement and velocity of the damped structure under random wind load or earthquake load. Marano and Greco [15] proposed some promising optimization criteria of TMD for vibration control considering stochastic excitation. In 2012, Tigli [16] derived the design formula of the analytic solution for mean square response minimization of structural velocity for the damped structure under random wind force. He further deduced the design formula of the approximate solution for mean square response minimization of displacement and acceleration. Over the past decades, the design of TMD systems has been widely investigated to mitigate various types of vibration problems [17–19]. The aforementioned design formulae [10–16] are derived from SDOF structures. However, in practical applications, most civil building structures are MDOF structures, which require simplifying an SDOF system to apply the TMD design formula. Furthermore, most of the design methods do not consider wind or seismic spectrum, which might result in a certain difference between the design scenario and the actual situation [4].

Since industrial development, there has been a continuous modification in the active control theory. Particularly, in the 1980s, with the development of science and technology, the active control theory received significant attention in the civil engineering field. Soong and Manolis [20] used the optimal linear quadratic regulator (LQR) theory to discuss the vibration reduction performance of a structure equipped with an actively controlled tendon system. Chung et al. [21] first used the shaking table test of an actively controlled tendon system to verify the feasibility of active control of structures. The Kajima Corporation in Japan first implemented active control technology in full-scale buildings [22]. With the gradual development of H_2 and H_∞ control theory [23], Spencer et al. [24] and Dyke et al. [25] applied the output feedback control theory to control a hydraulic-driven mass block installed on a building structure. Their results validated the feasibility and effectiveness of the output feedback active control theory.

Meanwhile, studies that employed active control theory to solve the optimal design problem of passive systems are also developing. Agrawal and Yang [26] modified the LQR control method to a constrained static output LQR and applied to design the parameters of the passive energy dissipation system. The optimal parameters within the gain matrix can be solved by constrained gradient optimization method. Furthermore, Yang et al. [27], using the linear matrix inequalities (LMI) framework, proposed an optimal methodology to design the passive energy dissipation devices, so that the design results can minimize the H_2 or H_∞ performance without simulating structural responses. Zuo and Nayfeh [28–30] used the output feedback control theory for designing a passive system by importing appropriate constraint conditions. The constrained conditions and gradient descent were used to obtain the optimal design parameters. Michielsen et al. [31] used the LQR-based optimization to obtain the optimal parameters of multiple tuned mass–spring–damper systems to reduce the plate vibration. Chang et al. [32, 33] transformed the optimization TMD design problem into an optimal observer problem to perform a parameter optimization design. For optimizing the negative stiffness and additional damping in a shear frame structure, Qu et al. [34] formulated the optimal problem as a static decentralized control and solved the parameters along a homotopy path. This iterative procedure enables the gain matrix to be merged with a specific load pattern. Broadly speaking, employing active control theory to obtain optimal design parameters of passive system has been proven to be a feasible approach [26–34]. However, most of the research has formulated the optimization problem to a sparse gain matrix [28–31, 34] because of applying a state feedback loop. This sparsity constraint is the key issue that raises the difficulties of finding the optimal solution.

The objective of this study is to propose a general optimal design method for a passive TMD using a static output feedback algorithm and an updating iterative procedure. The updating process utilizes the fact that the solution of static output feedback ensures an improved system response, enabling the gain matrix to converge without requiring the gradient of the objective function. Additionally, excitation shaping filters such as wind or seismic spectrum can be incorporated into the design scenario to ensure a comprehensive design. In this study, the equation of motion for

a MDOF structure that implemented with a designing passive TMD is reconfigured, so the optimal design problem of the TMD could be transformed into the nonsparse gain matrix optimization problem as static output feedback issue in active control field. The static output feedback algorithm is then applied to obtain the conditionally optimal gain matrix. Following that, the updating iterative procedure is further presented to determine the optimal TMD design parameters, thus the structural mean square or impulse responses reach the minimum without regarding the regulator of control authority. The feasibility of the proposed method is confirmed through numerical verification by comparing solutions obtained from the proposed method with the conventional analytic solutions. This study also employed the proposed method to obtain the optimal design parameters of TMD for the cases of velocity or absolute acceleration minimization of a SDOF structure subjected to earthquake loading. Finally, two cases of designing a passive TMD for MDOF structures considering wind or earthquake excitation shaping filter are also demonstrated.

2. Problem Formulation

2.1. Dynamics of a MDOF Building Structure Implemented with a TMD. If a N-DOF structure is implemented with a passive TMD, the DOF of the total system changes to $(N+1)$. The floor where the TMD is connected to the structure is the *j-th* floor ($j \le N$), as shown in Figure 1. The DOF of TMD is placed in the upper leftmost DOF of the matrices. The vector $\mathbf{d}$ can be configured using the TMD location as follows:

$$\mathbf{d}_{1\times(N+1)} = \begin{bmatrix} 1 & \mathbf{0}_{1\times(N-j)} & -1 & \mathbf{0}_{1\times(j-1)} \end{bmatrix}. \tag{1}$$

The equation of motion of the $(N+1)$-DOF system is expanded to

$$\mathbf{m}\ddot{\mathbf{x}}(t) + \mathbf{c}\dot{\mathbf{x}}(t) + \mathbf{k}\mathbf{x}(t) = \mathbf{e}\mathbf{w}_{\mathrm{f}}(t), \tag{2}$$

where $\mathbf{x}(t) = \begin{bmatrix} x_d(t) \\ \mathbf{x}_{\mathrm{s}}(t) \end{bmatrix}$ is the displacement vector, $x_d(t)$ and $\mathbf{x}_{\mathrm{s}}(t) = \begin{bmatrix} x_N(t) \\ \vdots \\ x_1(t) \end{bmatrix}$ are the displacement of TMD and structure relative to the base, respectively; $\mathbf{m} = \begin{bmatrix} m_d & \mathbf{0}_{1\times N} \\ \mathbf{0}_{N\times 1} & \mathbf{m}_{\mathrm{s}} \end{bmatrix}$ is the system mass matrix, m_d is the TMD mass, $\mathbf{m}_{\mathrm{s}}$ is the structural mass matrix of dimension $\mathbb{R}^{N\times N}$; $\mathbf{c} = c_d\mathbf{d}^T\mathbf{d} + \begin{bmatrix} 0 & \mathbf{0}_{1\times N} \\ \mathbf{0}_{N\times 1} & \mathbf{c}_{\mathrm{s}} \end{bmatrix}$ is the system damping matrix, c_d is the damping coefficient of TMD, $\mathbf{c}_{\mathrm{s}}$ is the structural damping matrix, and the superscript T denotes the transpose of the matrix; $\mathbf{k} = k_d\mathbf{d}^T\mathbf{d} + \begin{bmatrix} 0 & \mathbf{0}_{1\times N} \\ \mathbf{0}_{N\times 1} & \mathbf{k}_{\mathrm{s}} \end{bmatrix}$ is the system stiffness matrix, k_d is the stiffness of TMD, $\mathbf{k}_{\mathrm{s}}$ is the structural stiffness matrix; $\mathbf{w}_{\mathrm{f}}(t)$ and $\mathbf{e}$ are the external disturbance and the system external disturbance configuration matrix, respectively. If the external force is wind force, then $\mathbf{w}_{\mathrm{f}}(t) \in \mathbb{R}^{N\times 1}$ represents wind loads acting on each story of the structure. In addition, the TMD is mostly installed indoors, there is no direct wind action so $\mathbf{e} = \begin{bmatrix} \mathbf{0}_{1\times N} \\ \mathbf{I}_{N\times N} \end{bmatrix}$. If the external disturbance is the base acceleration, $\mathbf{w}_{\mathrm{f}}(t) \in \mathbb{R}^{1\times 1}$ is ground acceleration. The TMD is affected by the earthquake force as well, so $\mathbf{e} = -\mathbf{m}\mathbf{1}$ and $\mathbf{1} \in \mathbb{R}^{(N+1)\times 1}$ are the column vectors where the elements are ones.

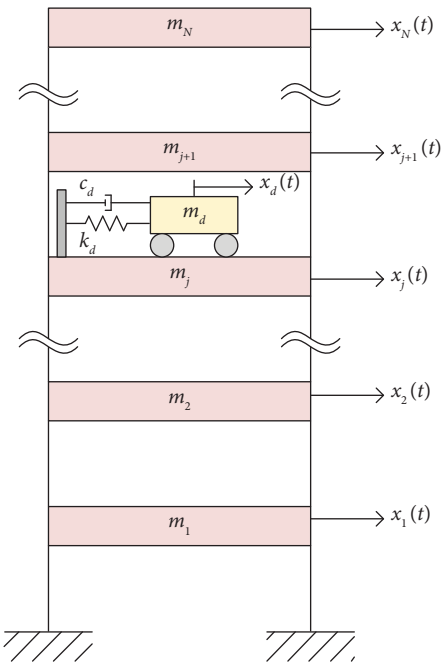

Figure 1: Schematic diagram of a MDOF structure equipped with a TMD.

2.2. Transformation of an Optimal Design Problem to Optimal Control Problem. To determine the optimal design of the TMD stiffness and damping coefficient and to maintain the overall system stability in the design process, which uses the active control algorithm, the stiffness and damping coefficient of TMD are set as

$$k_d = k_{d0} + k_{d1}, \tag{3}$$

$$c_d = c_{d0} + c_{d1}, \tag{4}$$

where k_{d0} and k_{d1} are the initial stiffness and controlling stiffness, respectively; c_{d0} and c_{d1} are the initial damping coefficient and controlling damping coefficient, respectively. To keep the system stable, the initial k_{d0} must be greater than 0 to ensure stability. A simple suggested value can be $m_d(2\pi f_s)^2$ which means the TMD is initially tuned to the natural frequency of the structure, f_s. The initial damping coefficient c_{d0} should be set as a positive value greater than 0. This makes the overall system asymptotically stable. The initial damping ratio is suggested to be about 1% or more. The sum of the restoring force and damping force of TMD is the partial interaction force of TMD and structure and is expressed as

$$u(t) = k_{d1}\left(x_d - x_j\right) + c_{d1}\left(\dot{x}_d - \dot{x}_j\right). \tag{5}$$

This interaction force $u(t)$ can be regarded as a control force requiring optimal design. The feedback signals of equation (5) are the TMD stroke and the velocity of TMD relative to the structure, so the controlling stiffness k_{d1} and controlling damping coefficient c_{d1} are the gains of this control force.

Substituting equation (3) to equation (5) into equation (2), the equation of motion of the system in configuration space changes to

$$\mathbf{m}\ddot{\mathbf{x}}(t) + \overline{\mathbf{c}}\dot{\mathbf{x}}(t) + \overline{\mathbf{k}}\mathbf{x}(t) = \mathbf{b}u(t) + \mathbf{e}\mathbf{w}_{\mathrm{f}}(t), \tag{6}$$

where $\overline{\mathbf{c}} = c_{d0}\mathbf{d}^T\mathbf{d} + \begin{bmatrix} 0 & \mathbf{0}_{1\times N} \\ \mathbf{0}_{N\times 1} & \mathbf{c}_{\mathrm{s}} \end{bmatrix}$ and $\overline{\mathbf{k}} = k_{d0}\mathbf{d}^T\mathbf{d} + \begin{bmatrix} 0 & \mathbf{0}_{1\times N} \\ \mathbf{0}_{N\times 1} & \mathbf{k}_{\mathrm{s}} \end{bmatrix}$ are the damping matrix and stiffness matrix, respectively, of the left part of the equation. $\mathbf{b} = -\mathbf{d}^T$ is the location vector of the control force. For convenient active control design, the equation of motion of equation (6) can be converted to the state-space expression as follows:

$$\dot{\mathbf{z}}_{\mathrm{s}}(t) = \mathbf{A}_{\mathrm{s}}\mathbf{z}_{\mathrm{s}}(t) + \mathbf{B}_{\mathrm{s}}u(t) + \mathbf{E}_{\mathrm{s}}\mathbf{w}_{\mathrm{f}}(t), \tag{7}$$

where $\mathbf{z}_{\mathrm{s}}(t) = \begin{bmatrix} \mathbf{x}(t) \\ \dot{\mathbf{x}}(t) \end{bmatrix}$ is the state vector; $\mathbf{A}_{\mathrm{s}} = \begin{bmatrix} \mathbf{0} & \mathbf{I} \\ -\mathbf{m}^{-1}\overline{\mathbf{k}} & -\mathbf{m}^{-1}\overline{\mathbf{c}} \end{bmatrix}$ is the system matrix; $\mathbf{B}_{\mathrm{s}} = \begin{bmatrix} \mathbf{0}_{(N+1)\times 1} \\ \mathbf{m}^{-1}\mathbf{b} \end{bmatrix}$ is the state-space control force location vector; $\mathbf{E}_{\mathrm{s}}$ is the state-space external force location matrix. It is expressed as $\mathbf{E}_{\mathrm{s}} = \begin{bmatrix} \mathbf{0}_{(N+1)\times N} \\ \mathbf{m}^{-1}\mathbf{e} \end{bmatrix}$ for an external wind force of multiple inputs or as $\mathbf{E}_{\mathrm{s}} = \begin{bmatrix} \mathbf{0}_{(N+1)\times 1} \\ \mathbf{m}^{-1}\mathbf{e} \end{bmatrix}$ for an external earthquake force of single input. The control force of equation (5) in the state-space form can be expressed as

$$u(t) = \begin{bmatrix} k_{d1} & c_{d1} \end{bmatrix} \begin{bmatrix} \mathbf{d} & \mathbf{0}_{1\times(N+1)} \\ \mathbf{0}_{1\times(N+1)} & \mathbf{d} \end{bmatrix} \begin{bmatrix} \mathbf{x} \\ \dot{\mathbf{x}} \end{bmatrix} = \mathbf{G}\mathbf{V}_{\mathrm{s}}\mathbf{z}_{\mathrm{s}}(t), \tag{8}$$

where $\mathbf{G} = \begin{bmatrix} k_{d1} & c_{d1} \end{bmatrix}$ is the undetermined gain matrix, including all the parameters to be designed for TMD (stiffness and damping coefficient), which is not a sparse gain matrix. The TMD relative state output matrix $\mathbf{V}_{\mathrm{s}} = \begin{bmatrix} \mathbf{v}_{\mathrm{rd}} \\ \mathbf{v}_{\mathrm{rv}} \end{bmatrix}$ is the matrix of the corresponding output vector combination, where $\mathbf{v}_{\mathrm{rd}} = \begin{bmatrix} \mathbf{d} & \mathbf{0}_{1\times(N+1)} \end{bmatrix}$ is the output vector of TMD displacement relative to the structure, and $\mathbf{v}_{\mathrm{rv}} = \begin{bmatrix} \mathbf{0}_{1\times(N+1)} & \mathbf{d} \end{bmatrix}$ is the output vector of TMD velocity relative to the structure. The relationship between the gain matrix and feedback signal of the structural system and partial interaction force is shown in Figure 2.

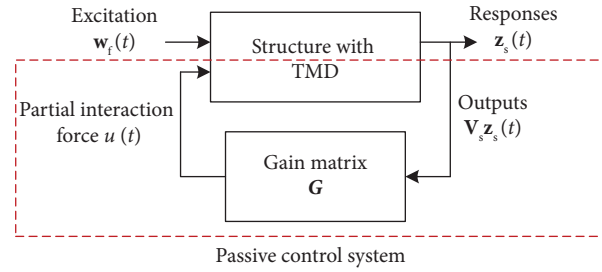

Figure 2: A schematic diagram of the gain matrix and output feedback signal of control force.

The state-space expression, besides the system state equation of equation (7), is often accompanied by an output (measurement) equation. The relation of the state $\mathbf{z}_{\mathrm{s}}(t)$, input $u(t)$, and output $\mathbf{y}_{\mathrm{s}}(t)$ of the system is usually expressed as

$$\mathbf{y}_{\mathrm{s}}(t) = \mathbf{C}_{\mathrm{s}}\mathbf{z}_{\mathrm{s}}(t) + \mathbf{D}_{\mathrm{s}}u(t) + \mathbf{F}_{\mathrm{s}}\mathbf{w}_{\mathrm{f}}(t), \tag{9}$$

where $\mathbf{y}_{\mathrm{s}}(t)$ is the output, which can be a single output or multiple outputs; $\mathbf{C}_{\mathrm{s}}$ is the output matrix; $\mathbf{D}_{\mathrm{s}}$ is the control force feedforward matrix; $\mathbf{F}_{\mathrm{s}}$ is the external disturbance feedforward matrix. $\mathbf{C}_{\mathrm{s}}$, $\mathbf{D}_{\mathrm{s}}$, and $\mathbf{F}_{\mathrm{s}}$ matrices can be selected according to the desired output.

2.3. Augment State-Space System with Excitation Shaping Filter. In the TMD design, the external excitation is often considered a random disturbance. However, it is also possible to consider the wind or earthquake characteristics in the modeling, i.e., the rational linearized Davenport spectrum [35] or Kanai–Tajimi spectrum [33]. The wind or seismic spectrum can be regarded as a shaping filter as

$$\begin{aligned} \dot{\mathbf{z}}_{\mathrm{f}}(t) &= \mathbf{A}_{\mathrm{f}}\mathbf{z}_{\mathrm{f}}(t) + \mathbf{E}_{\mathrm{f}}\mathbf{w}(t), \\ \mathbf{w}_{\mathrm{f}}(t) &= \mathbf{C}_{\mathrm{f}}\mathbf{z}_{\mathrm{f}}(t) + \mathbf{F}_{\mathrm{f}}\mathbf{w}(t), \end{aligned} \tag{10}$$

where $\mathbf{z}_{\mathrm{f}}(t)$ is the implicit states of the filter; $\mathbf{A}_{\mathrm{f}}$, $\mathbf{E}_{\mathrm{f}}$, $\mathbf{C}_{\mathrm{f}}$, and $\mathbf{F}_{\mathrm{f}}$ are the state-space matrices of the filter; $\mathbf{w}(t)$ is white-noise input and $\mathbf{w}_{\mathrm{f}}(t)$ is now a shaped external disturbance output which will continuously feed into the main system. The excitation shaping filter can be easily combined with the MDOF structure with the TMD system of equation (7) written in state-space representation by

$$\dot{\mathbf{z}}(t) = \mathbf{A}\mathbf{z}(t) + \mathbf{B}u(t) + \mathbf{E}\mathbf{w}(t), \tag{11}$$

where $\mathbf{z}(t) = \begin{bmatrix} \mathbf{z}_{\mathrm{s}}(t) \\ \mathbf{z}_{\mathrm{f}}(t) \end{bmatrix}$ is the states of the augment system; $\mathbf{A} = \begin{bmatrix} \mathbf{A}_{\mathrm{s}} & \mathbf{E}_{\mathrm{s}}\mathbf{C}_{\mathrm{f}} \\ \mathbf{0} & \mathbf{A}_{\mathrm{f}} \end{bmatrix}$, $\mathbf{B} = \begin{bmatrix} \mathbf{B}_{\mathrm{s}} \\ \mathbf{0} \end{bmatrix}$ and $\mathbf{E} = \begin{bmatrix} \mathbf{E}_{\mathrm{s}}\mathbf{F}_{\mathrm{f}} \\ \mathbf{E}_{\mathrm{f}} \end{bmatrix}$ are the system matrices of the augment system. The accompanied output equation of equation (9) becomes

$$\mathbf{y}(t) = \mathbf{C}\mathbf{z}(t) + \mathbf{D}u(t) + \mathbf{F}\mathbf{w}(t), \tag{12}$$

where $\mathbf{C} = [\,\mathbf{C}_s \;\; \mathbf{F}_s\mathbf{C}_f\,]$; $\mathbf{D} = \mathbf{D}_s$; and $\mathbf{F} = \mathbf{F}_s\mathbf{F}_f$. Moreover, the control force of equation (8) is now written as

$$u(t) = \mathbf{GV}\mathbf{z}(t), \tag{13}$$

where $\mathbf{V} = [\,\mathbf{V}_s \;\; \mathbf{0}\,]$ can be derived. The relationship of the augment system between the excitation shaping filter and passive control system is shown in Figure 3

If designing the TMD under random (white-noise) exicration is considered, then a constant of one is used for the shaping filter. As a result, the augment system can be simplified as $\mathbf{z}(t) = \mathbf{z}_s(t)$, $\mathbf{A} = \mathbf{A}_s$, $\mathbf{B} = \mathbf{B}_s$, $\mathbf{E} = \mathbf{E}_s$, $\mathbf{C} = \mathbf{C}_s$, and $\mathbf{F} = \mathbf{F}_s$.

3. Optimal Design of a Passive Tuned Mass Damper

According to equation (13), the partial interation force of TMD is not full-state feedback. The optimal gain matrix cannot be obtained by computing the expanded Riccati equation. This optimal gain matrix can be obtained by the static output feedback (direct output feedback) design method.

3.1. Optimal Design of the Static Output Feedback. Static output feedback is a method to design an active control force [36, 37]. It uses output feedback instead of state feedback. The control effect of static output feedback is usually not identical to the traditional LQR optimization in active control, because the initial conditions and constrains of control force have to be considered. However, these constraint conditions make the static output feedback suitable to apply for the passive system.

In control theory, the control force applied to the system aims to enhance the dynamic characteristics of the system and reduce its response when encountering external forces, so equation (13) is substituted in equation (11) to obtain

$$\dot{\mathbf{z}}(t) = [\mathbf{A} + \mathbf{BGV}]\mathbf{z}(t) + \mathbf{E}\mathbf{w}(t). \tag{14}$$

If the system is stationary and the external force $\mathbf{w}(t)$ is an impulse load at a time $t = 0$, this external impulse can be transformed into the initial condition of the system while satisfying the following equation:

$$\dot{\mathbf{z}}(t) = [\mathbf{A} + \mathbf{BGV}]\mathbf{z}(t), \mathbf{z}(0) = \mathbf{E}\overline{\mathbf{I}}, \tag{15}$$

where $\overline{\mathbf{I}}$ is the column vector of ones and the dimension is the number of external forces. The corresponding output of the solution can be expressed as

$$\mathbf{y}(t) = \mathbf{C}\mathbf{z}(t) + \mathbf{D}u(t), \mathbf{z}(0) = \mathbf{E}\overline{\mathbf{I}}. \tag{16}$$

To obtain the optimal gain matrix $\mathbf{G}$ to minimize equation (16), the quadratic effectiveness objective function J of output $\mathbf{y}(t)$ minimization is set up as

$$\begin{aligned} J &= \int_0^\infty \left[\mathbf{y}^T(t)\mathbf{y}(t)\right]\mathrm{d}t \\ &= \int_0^\infty \left[\mathbf{z}^T(t)\mathbf{Q}\mathbf{z}(t) + 2\mathbf{z}^T(t)\mathbf{N}u(t) + u^T(t)\mathbf{R}u(t)\right]\mathrm{d}t, \end{aligned} \tag{17}$$

where the weighting matrices in previous equation are as follows:

$$\mathbf{Q} = \mathbf{C}^T\mathbf{C}, \tag{18}$$

$$\mathbf{N} = \mathbf{C}^T\mathbf{D}, \tag{19}$$

where $\mathbf{Q}$ is the positive semidefinite weighting matrix of the system state; $\mathbf{N}$ is the weighting matrix of state and the control force coupling term; $R = \mathbf{D}^T\mathbf{D}$ is the control force regulator. These weighting matrices can be determined only according to the optimization objective by combinations of the output matrix $\mathbf{C}$ and $\mathbf{D}$ of equation (12), so the design method is general for various design cases. The output matrices corresponding to different optimization objectives are shown in Table 1. As presented in Table 1, the wind and earthquake forces are not distinguished because of the same output matrix in the same design objective under impulse excitation.

The objective function of equation (17) must follow the dynamics of the system and satisfy the constraint conditions. The constraint objective function $\overline{J}'$ can be derived by Lagrange multiplier $\mathbf{L}$ (Appendix A). The minimization of the constraint objective function is the simultaneous solution of partial derivatives of all the independent variables in $\overline{J}'$ to be 0 to obtain

$$\frac{\partial \overline{J}'}{\partial \mathbf{L}} = (\mathbf{A} + \mathbf{BGV})^T\mathbf{H} + \mathbf{H}(\mathbf{A} + \mathbf{BGV}) + \left(\mathbf{Q} + 2\mathbf{NGV} + \mathbf{V}^T\mathbf{G}^T R\mathbf{GV}\right) = \mathbf{0}, \tag{20a}$$

$$\frac{\partial \overline{J}'}{\partial \mathbf{H}} = \mathbf{Z}_0 + \mathbf{L}(\mathbf{A} + \mathbf{BGV})^T + (\mathbf{A} + \mathbf{BGV})\mathbf{L} = \mathbf{0}, \tag{20b}$$

$$\frac{\partial \overline{J}'}{\partial \mathbf{G}} = 2\mathbf{B}^T\mathbf{HLV}^T + 2\mathbf{N}^T\mathbf{LV}^T + 2R\mathbf{GVLV}^T = \mathbf{0}, \tag{20c}$$

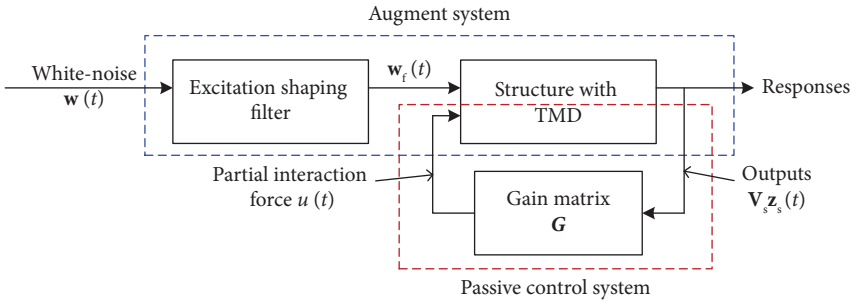

Figure 3: A schematic diagram of the augment system and passive control system.

Table 1: Output matrices corresponding to optimization objectives.

	Output target	Output matrix
(A)	The i-th floor displacement of the structure	$\mathbf{C}_s = \left[\bar{\mathbf{d}}\ \ \mathbf{0}_{1\times(N+1)}\right]$, $\mathbf{D}_s = [0]$
(B)	The i-th floor velocity of the structure	$\mathbf{C}_s = \left[\mathbf{0}_{1\times(N+1)}\ \ \bar{\mathbf{d}}\right]$, $\mathbf{D}_s = [0]$
(C)	The i-th floor acceleration of the structure	$\mathbf{C}_s = \bar{\mathbf{d}}\left[-\mathbf{m}^{-1}\bar{\mathbf{k}}\ \ -\mathbf{m}^{-1}\bar{\mathbf{c}}\right]$, $\mathbf{D}_s = \bar{\mathbf{d}}\mathbf{m}^{-1}\mathbf{b}$
(D)	The i-th model displacement of the structure	$\mathbf{C}_s = \left[0\ \ \Phi_{1\times N}\ \ \mathbf{0}_{1\times(N+1)}\right]$, $\mathbf{D}_s = [0]$

$\bar{\mathbf{d}} = \left[\mathbf{0}_{1\times(N+1-i)}\ \ 1\ \ \mathbf{0}_{1\times(i-1)}\right]$ is the i-th floor output location vector of the structure. $\Phi_{1\times N}$ is the i-th mode shape of the bare structure.

The algebraic equations of equations (20a)–(20c) are solved simultaneously to obtain the gain matrix $\mathbf{G}$. Usually, solving the algebraic equations of equations (20a)–(20c) simultaneously can be iterative [38, 39] by regarding the equations (20a) and (20b) as Lyapunov equations. The solution of the Lyapunov equation of equations (20a) and (20b) is shown in Appendix B.

Furthermore, the solution of equation (20b) is related to the initial condition of the system. Unlike [26, 36], that uses the identity matrix as the quadratic initial condition matrix, the quadratic initial condition matrix is related to the external disturbance location matrix, i.e., $\mathbf{Z}_0 = \mathbf{E}\bar{\mathbf{I}}\bar{\mathbf{I}}^T\mathbf{E}^T$ (Appendix A). Therefore, the quadratic initial condition matrix under wind or earthquake forces is different, as shown in Table 2.

In addition to the output matrices listed in Table 1, further output matrices of specific objectives can be combined as required.

3.2. Updating Iterative Procedure. However, when output matrix $\mathbf{D}$ is zero in some cases, then the regulator R is zero so there is no solution that consists of the Lyapunov equations [38, 39]. Then, equations (20a)–(20c) is not easy to solve. Therefore, a conditional objective is used to replace equation (17) as follows:

$$J_c = \int_0^\infty \left[\mathbf{y}^T(t)\mathbf{y}(t) + u^T(t)\bar{R}u(t)\right]\mathrm{d}t, \tag{21}$$

where $\bar{R}$ is an assigned control force regulator. To minimize equation (21), the partial derivatives are the same as equations (20a)–(20c) except that the control regulator in equations (20a)–(20c) becomes

$$R = \mathbf{D}^T\mathbf{D} + \bar{R}. \tag{22}$$

If the gain matrix $\mathbf{G}$ is obtained by minimizing equation (21) which is a conditional weight balanced optimal solution of output $y(t)$ and control force $u(t)$, then the performance will not be as well as the optimal solution of equation (17). Therefore, this paper further presents an updating iterative procedure to obtain the optimal design value that minimization of equation (17) is achieved.

Once the gain matrix $\mathbf{G} = \left[k_{d1}\ \ c_{d1}\right]$ calculated by static output feedback of equations (20a)–(20c) is a conditionally optimal gain matrix that can always improve the dynamic response of the system but not reach the overall optimum, the controlling stiffness k_{d1} and controlling damping coefficient c_{d1} can be used to update the initial stiffness k_{d0} and initial damping coefficient c_{d0} of the TMD as follows:

$$k_{d0} \overset{\text{updating by}}{\longrightarrow} k_{d0} + k_{d1}, \tag{23}$$

$$c_{d0} \overset{\text{updating by}}{\longrightarrow} c_{d0} + c_{d1}. \tag{24}$$

The corresponding matrices, such as $\bar{\mathbf{c}}$, $\bar{\mathbf{k}}$ and state-space matrices, are therefore updated collectively. After the TMD design parameters in the system matrix (k_{d0} and c_{d0}) are

Table 2: External force types and corresponding quadratic initial condition matrix.

	External force type	External disturbance configuration matrix	State-space external disturbance location matrix	Column vector of ones	Quadratic initial condition matrix
(i)	Wind force $\mathbf{w}_f(t) \in \mathbb{R}^{N\times 1}$ (multiple input)	$\mathbf{e} = \begin{bmatrix} \mathbf{0}_{1\times N} \\ \mathbf{I}_{N\times N} \end{bmatrix}$	$\mathbf{E}_s = \begin{bmatrix} \mathbf{0}_{(N+1)\times N} \\ \mathbf{m}^{-1}\mathbf{e} \end{bmatrix}$	$\overline{\mathbf{1}} = \begin{bmatrix} 1 \\ \vdots \\ 1 \end{bmatrix}$	$\mathbf{Z}_0 = \mathbf{E}\overline{\mathbf{1}}\overline{\mathbf{1}}^T\mathbf{E}^T$
(ii)	Earthquake $\mathbf{w}_f(t) \in \mathbb{R}^{1\times 1}$ (single input)	$\mathbf{e} = -\mathbf{m}\mathbf{1}$	$\mathbf{E}_s = \begin{bmatrix} \mathbf{0}_{(N+1)\times 1} \\ \mathbf{m}^{-1}\mathbf{e} \end{bmatrix}$	$\overline{\mathbf{1}} = 1$	

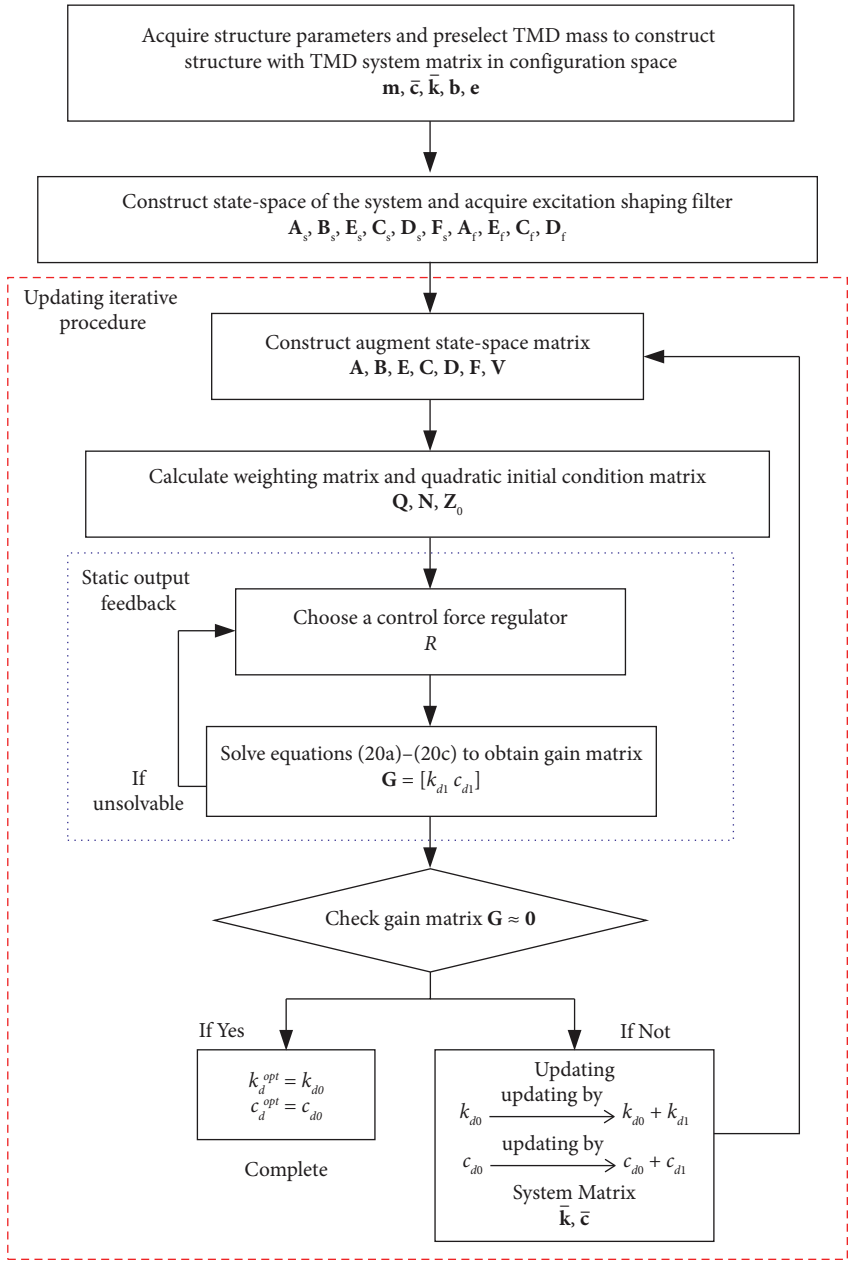

Figure 4: The flow chart of a designing optimal TMD by static output feedback and updating iterative procedure.

updated by the obtained gain matrix, a newly conditionally gain matrix **G** can be recalculated by static output feedback to process a new update.

Through an iterative updating operation, the conditionally gain matrix **G** must converge and approach **0** or smaller than a positive microvalue ε ($k_{d1} \approx 0$ and $c_{d1} \approx 0$). This means that even if the control force is applied, a better objective function cannot be obtained through the static output feedback. Particularly, the TMD design parameters (k_{d0} and c_{d0}) in the system matrix are now updated to the optimal design parameters because the controlling stiffness k_{d1} and controlling damping coefficient c_{d1} are zeros. Therefore, the iterative operation is complete.

3.3. General Optimal Design Method of a Passive Tuned Mass Damper. The iterative procedure combined with static output feedback is as follows:

(1) Given the structural parameters $\mathbf{m}_s$, $\mathbf{c}_s$, $\mathbf{k}_s$, and TMD mass m_d, the initial stiffness k_{d0} and damping coefficient c_{d0} of TMD are determined. The system matrices **m**, $\bar{\mathbf{c}}$, $\bar{\mathbf{k}}$, **b,** and **e** in configuration space are subsequently constructed.

(2) The state-space matrices $\mathbf{A}_s$, $\mathbf{B}_s$, $\mathbf{E}_s$ are established. The output matrices $\mathbf{C}_s$ and $\mathbf{D}_s$ (Table 1) and the corresponding output vector $\mathbf{V}_s$ are determined. Furthermore, the excitation shaping filter is selected or omitted as required.

(3) The augment state-space system matrices according to equations (11)–(13) are constructed.

(4) The weighting matrices, $\mathbf{Q}$ and $\mathbf{N}$, and the initial condition $\mathbf{Z}_0$ are calculated according to equations (18) and (19) and Table 2.

(5) A regulator weight R for the weighting $\overline{R}$ is selected.

(6) Equations (20a)–(20c) of static output feedback is solved simultaneously to obtain a conditionally optimal gain matrix $\mathbf{G} = \begin{bmatrix} k_{d1} & c_{d1} \end{bmatrix}$. If simultaneous solving fails, we return to Step 5 to modify regulator weight R.

(7) Each element of the conditionally optimal gain matrix $\mathbf{G}$ is examined that approaches 0 (i.e., smaller than ε). If any element does not approach 0, updating of k_{d0} and c_{d0} in $\overline{\mathbf{c}}$ and $\overline{\mathbf{k}}$ is proceeded using equations (23) and (24), and then return to Step 3. Conversely, if all elements approach 0, the optimal design parameters of TMD are determined as $k_d^{\text{opt}} = k_{d0}$ and $c_d^{\text{opt}} = c_{d0}$, and the design procedure is completed.

The proposed design procedure is compiled in Figure 4.

It is worth remarking that the gain matrix solving by static output feedback is not a sparse gain matrix and its elements are just equal to the undetermined TMD design parameters. In the iterative process, the updating gain matrix $\mathbf{G}$ always converges toward zero. This is because the solution of static output feedback ensures that the obtained gain matrix always improves the system response. The required control effort reduces after the updating. Therefore, even though the gradient of the objective function of every step is not calculated in the iterative process, the presented updating method is workable.

Furthermore, the selection of the regulator R of static output feedback is only related to iterative convergence speed but not to the finalized optimal design value. This is also because the gain matrix $\mathbf{G}$ is converged to zero eventually in the updating procedure, so the role of the regulator R in static output feedback is diminished. The control effort is reduced during the iterative process; therefore, as long as the value of R is selected appropriately such that the simultaneous solution of equations (20a)–(20c) is available, the regulator R is unnecessary to change in the subsequent iterative process.

In the iterative procedure, the R is first recommended to attempt a small positive value. Usually, there is no simultaneous solution when choosing a too-small value of R for equation (20a); therefore, the R-value can choose a small value for first attempt and then be gradually enlarged until the solution of equation (20a) is available. Thus, an appropriate regulator R to make a faster convergence of iterative procedure can be obtained.

The limitation of the proposed method is that the static output feedback control algorithm is used to design a linear time-invariant (LTI) system, so the structural mass, damping, and stiffness are unvaried during the design process. To apply the proposed method to design a linear TMD on a nonlinear structure, an equivalent linearized structural model must be adopted first.

4. Validation of SDOF Structure Implemented with a Tuned Mass Damper

Taking a SDOF structure implemented with the TMD as an example, after the TMD is installed, it is a 2-DOF system. The TMD location vector $\mathbf{d} = \begin{bmatrix} 1 & -1 \end{bmatrix}$, the system displacement vector $\mathbf{x}(t) = \begin{bmatrix} x_d(t) \\ x_s(t) \end{bmatrix}$, the mass matrix $\mathbf{m} = \begin{bmatrix} m_d & 0 \\ 0 & m_s \end{bmatrix}$, the damping matrix $\overline{\mathbf{c}} = \begin{bmatrix} c_{d0} & -c_{d0} \\ -c_{d0} & c_{d0} + c_s \end{bmatrix}$, and the stiffness matrix $\overline{\mathbf{k}} = \begin{bmatrix} k_{d0} & -k_{d0} \\ -k_{d0} & k_{d0} + k_s \end{bmatrix}$ are considered. $\mathbf{e}$ is the external force disturbance vector. If the external force on the system is wind force, then $\mathbf{e} = \begin{bmatrix} 0 \\ 1 \end{bmatrix}$. If the external force is an earthquake force, then $\mathbf{e} = \begin{bmatrix} -m_d \\ -m_s \end{bmatrix}$. The equation of motion of equation (6) can be established according to the corresponding system matrices.

The equation of motion is transformed into state-space expression and expressed as equation (7). In this section, the excitation shaping filter is neglected so that the external disturbance is considered a random excitation. Then, the system state is expanded to $\mathbf{z}_s{}^T(t) = \begin{bmatrix} x_d(t) & x_s(t) & \dot{x}_d(t) & \dot{x}_s(t) \end{bmatrix}$. In equation (8), the active control force is $u(t) = \mathbf{G}\mathbf{V}_s\mathbf{z}_s(t)$ where $\mathbf{G} = \begin{bmatrix} k_{d1} & c_{d1} \end{bmatrix}$ is the undetermined gain matrix. TMD relative displacement configuration vector is expressed as $\mathbf{v}_{\text{rd}} = \begin{bmatrix} 1 & -1 & 0 & 0 \end{bmatrix}$, and TMD relative velocity configuration vector is expressed as $\mathbf{v}_{\text{rv}} = \begin{bmatrix} 0 & 0 & 1 & -1 \end{bmatrix}$, so the TMD relative state output matrix is $\mathbf{V}_s = \begin{bmatrix} 1 & -1 & 0 & 0 \\ 0 & 0 & 1 & -1 \end{bmatrix}$. The output location vector of the structure is expressed as $\overline{\mathbf{d}} = \begin{bmatrix} 0 & 1 \end{bmatrix}$, so the weighting matrices, $\mathbf{Q}$ and $\mathbf{N}$, of the objective function can be established according to different optimization objectives as shown in Table 1.

Warburton [12] and Korenev and Reznikov [13] proposed certain analytic solutions of a SDOF undamped structure implemented with TMD. Tigli [16] also proposed the analytic design formula for SDOF damped structure. These optimal design formulae aim at the objective mean square response minimization under random excitation, such as the minimization of the area under a specific frequency response function. According to static output feedback, the external disturbance assumes to be the impulse loading in the time domain during derivation. In addition, by Parseval's theorem, the H_2-norm optimization of the impulse function in the time domain is equal to the frequency response function in the frequency domain as follows:

$$\begin{aligned} \|H\|_2 &= \left[\int_0^\infty h^T(t) h(t) dt \right]^{1/2} \\ &= \left[\frac{1}{2\pi} \int_{-\infty}^{\infty} H^H(\omega) H(\omega) d\omega \right]^{1/2}, \end{aligned} \tag{25}$$

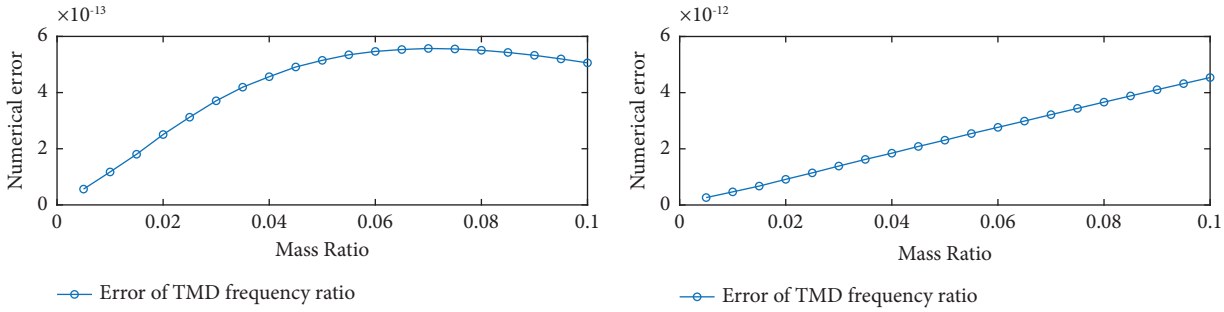

FIGURE 5: Numerical error of proposed method for the case of minimizing structural displacement under wind force: (a) error of optimal TMD frequency ratio, and (b) error of optimal TMD damping ratio.

where $h(t)$ is the impulse response of the system; $H(\omega)$ is the frequency response function of the system; the superscript ^{H} denotes the conjugate transpose of the matrix. Therefore, the optimal design method proposed in this paper is identical to the mean-square response minimization under random excitation if the excitation shaping filter is neglected. When designing the optimal design parameters of TMD of a SDOF structure, it should be equal to the analytic solution by [12, 13, 16].

The mass of the SDOF structure m_s is 29485 kg, and the structure frequency is assigned 0.5 Hz for numerical simulation. Expect for undamped structure, for the case of damped structure, the structural damping ratio is selected 0.05. To discuss the cases of different TMD mass ratios ($R_m = m_d/m_s$), the mass ratio variation range is 0.005~0.1. The common design parameters of TMD, i.e., optimal frequency ratio $R_f = f_d/f_s$ (f_d is the natural frequency of TMD) and the optimal damping ratio $\zeta_d = c_d/2\sqrt{m_d k_d}$ of TMD, are calculated for comparison. To obtain the optimal TMD design parameters under random disturbance, the excitation shaping filter is neglected in this section. After the optimal design parameters k_d^{opt} and c_d^{opt} of TMD are obtained by following the procedure of Figure 4, the optimal frequency ratio R_f^{opt} of TMD and the optimal damping ratio ζ_d^{opt} of TMD are further calculated. The numerical error of the obtained design parameters respected to the analytic solution is defined as

$$R_f^{\text{err}} = \left| R_f^{\text{opt}} - R_f^{\text{anal}} \right|, \tag{26.1}$$

$$\zeta_d^{\text{err}} = \left| \zeta_d^{\text{opt}} - \zeta_d^{\text{anal}} \right|, \tag{26.2}$$

where the analytic solutions of R_f^{anal} and ζ_d^{anal} can be obtained from [12, 13, 16].

The cases of (1) structural displacement or velocity minimization under wind force, (2) structural velocity minimization under wind force, (3) structural acceleration minimization under wind force, and (4) structural displacement minimization under earthquake forces are analyzed and compared with the analytic solutions of mean-square response minimization to verify the proposed method.

4.1. Structural Displacement and Velocity Minimization under White-Noise Wind Force. For the case of minimizing structural displacement of an undamped structure under wind force, the output vectors of structural displacement are $\mathbf{C} = [0\ 1\ 0\ 0]$ and $\mathbf{D} = [0]$. The system weighting matrix $\mathbf{Q} = \mathbf{C}^T\mathbf{C}$ and the weighting matrix of the coupling term $\mathbf{N} = \mathbf{C}^T\mathbf{D}$ can then be obtained accordingly by equations (18) and (19). The quadratic initial condition can also be obtained from Table 2, that is, $\mathbf{Z}_0 = \begin{bmatrix} 0 & 0 & 0 & 0 \\ 0 & 0 & 0 & 0 \\ 0 & 0 & 0 & 0 \\ 0 & 0 & 0 & 1/m_s^2 \end{bmatrix}$. After the corresponding matrices are established, a control force weight that the solution of equations (20a)–(20c) could be available is set up, e.g., $R = 10^{-5} \sim 10^{-7}$. The microvalue of the convergence condition is also assigned, e.g., $\varepsilon = 10^{-10}$. The errors of the obtained design parameters respected to Warburton's formula [12] are illustrated in Figure 5.

As shown in Figure 5, for the undamped structure, all the errors of the design parameters are extremely small. The optimal TMD parameters obtained by the proposed method can be regarded identical to the analytic solution proposed by Warburton [12].

In addition to minimizing structural velocity under wind force, the output vector is just changed as $\mathbf{C} = [0\ 0\ 0\ 1]$ so the output $\mathbf{y}(t)$ in equation (13) becomes structural velocity. The optimal TMD parameters can also be obtained by the proposed method. In this scenario, for undamped structures, the errors of the design parameters obtained by the proposed method are so small that they can be regarded as equal to the analytic solution proposed by Warburton [12]. For the damped structure, the errors of the obtained design parameters respected to Tigli's formulae [16] are illustrated in Figure 6. The errors are also quiet small. The optimal TMD parameters obtained by the proposed method can be regarded identical to the analytic solution proposed by Tigli [16]. The accuracy and feasibility of the proposed method are verified.

4.2. Structural Acceleration Minimization under White-Noise Wind Force. In this case, the output vectors of structural acceleration are $\mathbf{C} = [k_{d0}/m_s\ -(k_{d0}/m_s) - (k_s/m_s)(c_{d0}/m_s)-$

$(c_{d0}/m_s) - (c_s/m_s)]$ and $\mathbf{D} = [1/m_s]$. After the corresponding matrices are established, a control force weight, e.g., $R = 10^{-4} \sim 10^{-6}$ is set up. The microvalue of the convergence condition is also assigned, e.g., $\varepsilon = 10^{-10}$. Then, the optimal TMD parameters can be determined by using the method proposed in this paper. For the undamped structure, Figure 7 shows the errors of optimal parameters obtained by the proposed method with respect to the modified solution proposed by Korenev and Reznikov [13] (Appendix C). The optimal TMD parameters obtained by the proposed method show that the results exhibit well consistency with the analytic solutions proposed by Korenev and Reznikov [13].

4.3. Structural Displacement Minimization under Random Earthquake Force. In the base excitation case, the output vectors of structural displacement are $\mathbf{C} = \begin{bmatrix} 0 & 1 & 0 & 0 \end{bmatrix}$ and $\mathbf{D} = [0]$, and the system weighting matrices $\mathbf{Q}$ and $\mathbf{N}$ can then be obtained by equations (18) and (19). The external disturbance is base acceleration, so the quadratic initial condition $\mathbf{Z}_0 = \begin{bmatrix} 0 & 0 & 0 & 0 \\ 0 & 0 & 0 & 0 \\ 0 & 0 & 1 & 1 \\ 0 & 0 & 1 & 1 \end{bmatrix}$ (Table 2). After the corresponding matrices are established, a control force weight that the solution of equations (20a)–(20c) could be available is set up, e.g., $R = 10^{-6} \sim 10^{-8}$. The microvalue of the convergence condition is also assigned, e.g., $\varepsilon = 10^{-10}$. Then, the optimal TMD parameters can be obtained by the proposed method.

For the undamped structure, the optimal parameters obtained by the proposed method are equal to the analytic solution proposed by Warburton [12]. Figure 8 shows the errors of optimal parameters obtained by the proposed method with respect to the Warburton's [12].

By comparing these cases with the mentioned references, the feasibility of the H_2-norm optimization according to the proposed method is validated.

5. Numerical Demonstration of Optimal Tuned Mass Damper Design Problems

There is no explicit design formula available in reference to a SDOF structure implemented with a TMD for the H_2-norm minimization of velocity or absolute acceleration of the structure under impulse or random earthquake force. For these cases, the proposed method can provide the optimal TMD design parameters. The results are compiled as a design look-up tables over common range for engineers. The design method proposed in this paper can apply the optimal TMD design for the MDOF structure. Therefore, a MDOF structure equipped with the TMD is also verified for optimal design in this section.

5.1. Structural Velocity or Absolute Acceleration Minimization under Random Earthquake Force. To minimize the structural velocity of a SDOF structure implemented with a TMD subjected to the earthquake force, the output vectors of structural velocity are $\mathbf{C} = \begin{bmatrix} 0 & 0 & 0 & 1 \end{bmatrix}$ and $\mathbf{D} = [0]$. On the other hand, for the case of minimizing the absolute acceleration of the structure subjected to earthquake forces, the output vectors of absolute acceleration are $\mathbf{C} = [k_{d0}/m_s \;\; -(k_{d0}/m_s) - (k_s/m_s) \;\; (c_{d0}/m_s) \;\; -(c_{d0}/m_s) - (c_s/m_s)]$ and $\mathbf{D} = [1/m_s]$.

After the corresponding matrices $\mathbf{Q}$, $\mathbf{N}$ and $\mathbf{Z}_0$ are established, a control force weight R, for which the solution of equations (20a)–(20c) could be available, is selected. Then, the optimal TMD parameters to minimize structural velocity or absolute acceleration can be obtained separately using the proposed method. As a design reference for engineers, the parameters are listed in Tables 3 and 4.

It is worth mentioning that the effectiveness of a theory regarding the energy transferred from earthquake input to building structures during a single impulse has been demonstrated in revealing the characteristics of the energy transfer function [40]. In recent years, Akehashi and Takewaki [41, 42] have further proposed using double impulse or pseudomultiple impulse, considering the near-fault or resonance effect of long-duration excitations, to capture the critical response of structures.

5.2. Design of Optimal Tuned Mass Damper Installed on a 5 Stories Structure Subjected to Earthquake. In some cases, the MDOF structure cannot always be directly simplified to a SDOF structure, or the simplified SDOF is likely to have larger differences than the original MDOF structure. The proposed method applied for a MDOF structure subjected to earthquake is demonstrated in this section. An illustrated case of a 5-story structure [43] is presented in Figure 1. The mass matrix, damping matrix, and stiffness matrix of the structure are shown in Table 5. Notably, the stiffness matrix of the structure is a full matrix because the stiffness matrix sources are from system identification. The TMD is installed on the 4th floor. The design objective is to reduce the response of the top-floor slab of the structure under earthquake force.

Moreover, if the Kanai–Tajimi spectrum is used as the excitation shaping filter [44], where ω_g and ζ_g are the ground parameters of the filter, the state-space representation of the shaping filter is given as $\mathbf{A}_f = \begin{bmatrix} 0 & 1 \\ -\omega_g{}^2 & -2\zeta_g\omega_g \end{bmatrix}$; $\mathbf{B}_f = \begin{bmatrix} 0 \\ -1 \end{bmatrix}$; $\mathbf{C}_f = \begin{bmatrix} -\omega_g{}^2 & -2\zeta_g\omega_g \end{bmatrix}$ and $\mathbf{D}_f = [0]$.

After the TMD is installed on the 4th floor of the structure, the system becomes 6-DOF. The mass of the TMD is selected as 2.8 kg. The TMD location configuration vector $\mathbf{d}_{1\times6} = [1 \;\; 0 \;\; -1 \;\; 0 \;\; 0 \;\; 0]$. A scaled Kanai–Tajimi spectrum parameters for this case have $\omega_g = 15$ rad/s and $\zeta_g = 0.4$. The Kanai–Tajimi spectrum is shown in Figure 9.

If the optimization objective is to minimize the top-floor absolute acceleration response, the output matrices $\mathbf{C}_s = \overline{\mathbf{d}}\left[-\mathbf{m}^{-1}\overline{\mathbf{k}} \;\; -\mathbf{m}^{-1}\overline{\mathbf{c}}\right]$, $\mathbf{D}_s = \overline{\mathbf{d}}\mathbf{m}^{-1}\mathbf{b}$ and $R = 1.0$ are assigned. After applying the proposed method as shown in Figure 4, the obtained optimal stiffness of TMD k_d^{opt} is

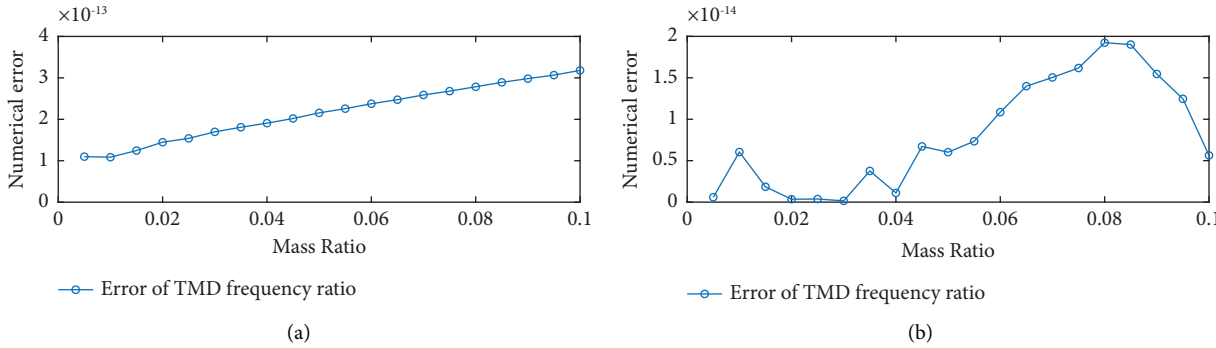

Figure 6: Numerical error of proposed method for the case of minimizing structural velocity under wind force: (a) error of optimal TMD frequency ratio, and (b) error of optimal TMD damping ratio.

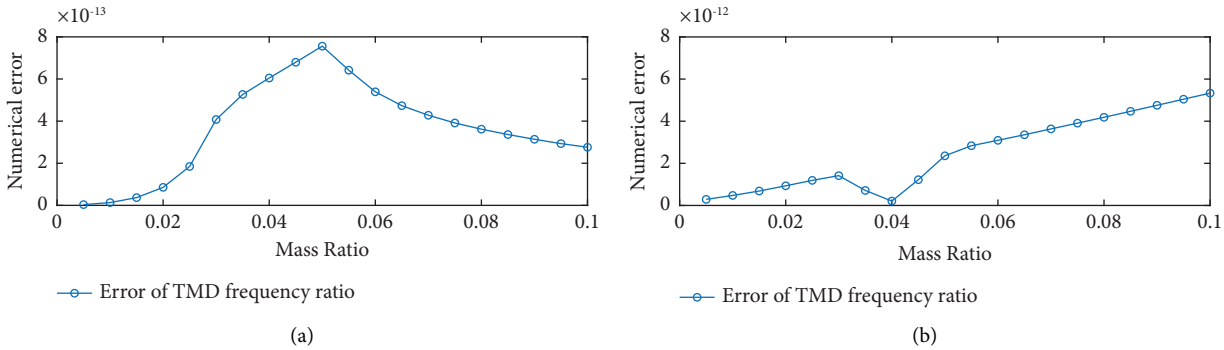

Figure 7: Numerical error of proposed method for the case of minimizing structural acceleration under wind force: (a) error of optimal TMD frequency ratio, and (b) error of optimal TMD damping ratio.

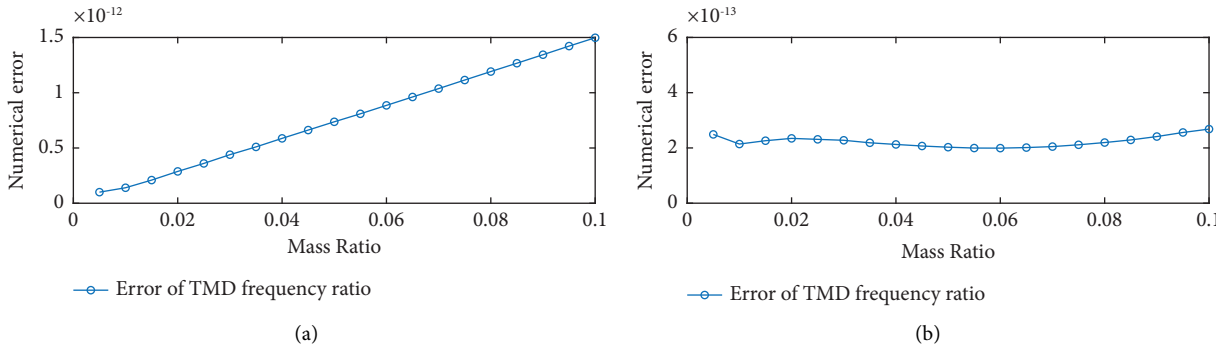

Figure 8: Numerical error of proposed method for the case of minimizing structural displacement under white-noise base excitation: (a) error of optimal TMD frequency ratio, and (b) error of optimal TMD damping ratio.

87.5943 N/m and the optimal damping coefficient c_d^{opt} is 3.3220 N-s/m. The design results are compared with Den Hartog's formulae [10]. As the frequency response function of the top-floor absolute acceleration is shown in Figure 10, the top-floor absolute acceleration of the first mode can be reduced effectively. The H_2-norm of the top-floor absolute acceleration is reduced to 11.3147 from 14.8156 in the case without TMD, which is slightly better than the design using Dan Hartog's formulae of 11.3306. Figure 11 shows the H_2-norm convergence versus the iteration steps of the illustrated case. As shown in Figure 11, the iteration converges after 171 steps. This verifies that the proposed method can be used in MDOF structure, and the TMD can be installed on any floor.

5.3. Design of Optimal Tuned Mass Damper Installed on a 60 Stories High-Rise Structure Subject to Wind Loads. A 60-story outrigger building, located on the St. Francis Shangri-La Palace in the Philippines, was chosen for the numerical study of a high-rise building incorporating a TMD subjected to wind loads. The structure has a height of 210 m and is

Table 3: Optimal TMD design parameters of structural velocity minimization under random earthquake force.

	Structural damping ratio ζ_s							
R_m	0		0.01		0.02		0.05	
	R_f	ζ_d	R_f	ζ_d	R_f	ζ_d	R_f	ζ_d
0.001	0.999001	0.015803	0.998428	0.015800	0.997656	0.015795	0.994176	0.015772
0.005	0.995025	0.035267	0.993874	0.035253	0.992528	0.035235	0.987350	0.035163
0.01	0.990099	0.049752	0.988524	0.049725	0.986758	0.049693	0.980347	0.049570
0.02	0.980392	0.070014	0.978239	0.069962	0.975900	0.069903	0.967817	0.069689
0.05	0.952381	0.109109	0.949178	0.108985	0.945806	0.108851	0.934735	0.108399
0.10	0.909091	0.150756	0.904905	0.150522	0.900574	0.150277	0.886778	0.149479

Table 4: Optimal TMD design parameters of absolute acceleration of the structure minimization under random earthquake force.

	Structural damping ratio ζ_s							
R_m	0		0.01		0.02		0.05	
	R_f	ζ_d	R_f	ζ_d	R_f	ζ_d	R_f	ζ_d
0.001	0.999251	0.015805	0.999093	0.015805	0.998937	0.015806	0.998505	0.015807
0.005	0.996268	0.035289	0.995919	0.035289	0.995573	0.035290	0.994592	0.035294
0.01	0.992571	0.049814	0.992082	0.049814	0.991599	0.049814	0.990223	0.049823
0.02	0.985282	0.070187	0.984604	0.070187	0.983935	0.070189	0.982030	0.070207
0.05	0.964212	0.109772	0.963199	0.109773	0.962203	0.109778	0.959381	0.109826
0.10	0.931541	0.152540	0.930231	0.152543	0.928949	0.152554	0.925341	0.152659

Table 5: System parameters of a 5-story structure [43].

Mass matrix $\mathbf{m}_s$ (kg)	$\begin{bmatrix} 19.57 & 0 & 0 & 0 & 0 \\ & 19.57 & 0 & 0 & 0 \\ & & 19.57 & 0 & 0 \\ & \text{sym.} & & 19.57 & 0 \\ & & & & 19.57 \end{bmatrix}$				
Damping matrix $\mathbf{c}_s$ (N-s/m)	$\begin{bmatrix} 15.93 & -14.28 & 0.11 & 0.46 & 0.06 \\ & 34.26 & -16.46 & -1.04 & 0.30 \\ & & 36.22 & -15.61 & -0.79 \\ & \text{sym.} & & 37.46 & -13.67 \\ & & & & 47.19 \end{bmatrix}$				
Stiffness matrix $\mathbf{k}_s$ (N/m)	$\begin{bmatrix} 14621 & -22962 & 7463 & 1169 & -211 \\ & 52688 & -36587 & 5481 & 1612 \\ & & 58344 & -35825 & 4549 \\ & \text{sym.} & & 58596 & -36564 \\ & & & & 77108 \end{bmatrix}$				
Modal frequencies $\mathbf{f}_s$ (Hz)	Mode 1 to 5				
	0.915	3.371	7.107	10.657	12.728
Modal damping ratios ζ_s	Mode 1 to 5				
	0.02				

modeled as a cantilever beam which includes 60 translational and 60 rotational DOFs (total 120 DOFs). The building has a total mass of 29,750 tons and the outrigger is not considered in this numerical study. The natural frequencies of the first three structural modes are 0.185 Hz, 1.145 Hz, and 3.146 Hz, respectively. The structural damping ratio of 0.01 is assumed for each mode under wind loads. For more details on the outrigger building, readers are suggested to refer to Chang et al. [45] and Wang et al. [9, 46]. The Davenport wind spectrum of the outrigger building was evaluated by Wang et al. [47]. To consider the Davenport wind spectrum as an excitation shaping filter, a 4-order rational transfer function is fitted as follows:

$$T(s) = \frac{9.371s^3 + 226.8s^2 + 801.96s + 7.294}{s^4 + 32.923s^3 + 174.35s^2 + 58.987s + 1.9937}. \tag{27}$$

Figure 12 illustrates the power spectrum of the Davenport spectrum and the fitted rational transfer function. The rational transfer function is subsequently converted to a state-space model, as shown in equation (10), enabling the

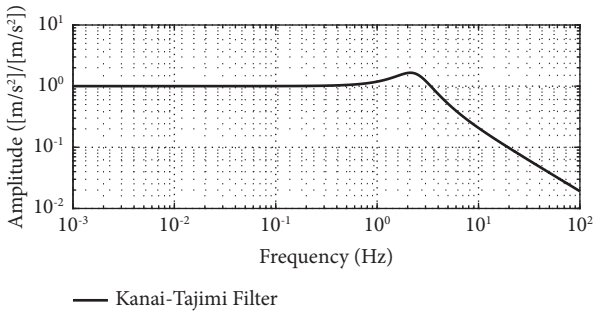

Figure 9: The selected Kanai–Tajimi spectrum for excitation shaping filter.

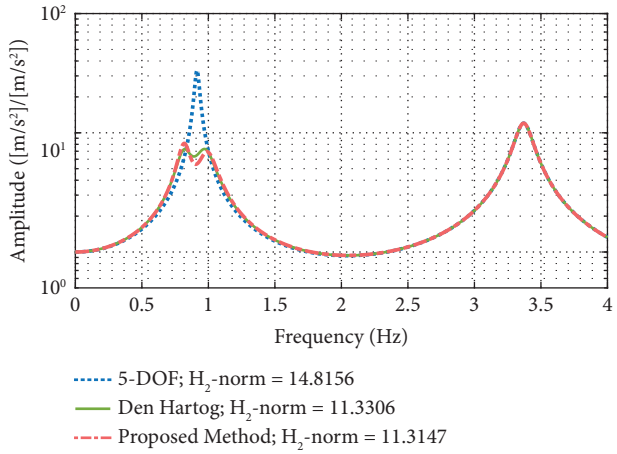

Figure 10: Top-floor absolute acceleration frequency response function of the 5-story structure.

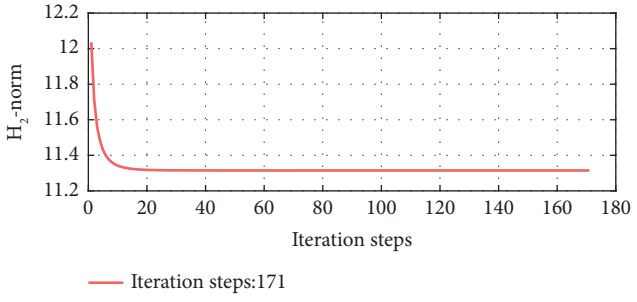

Figure 11: The H_2-norm convergence versus the iteration steps.

excitation shaping filter to be applied to each excitation input and combined with the MDOF structure incorporating the TMD system.

A TMD with a mass of 200 tons is installed on the top of the 60-story building. The mass ratio of the TMD with respect to the fundamental structural modal mass is approximately 2.7%. When the proposed method is applied to minimize the top-floor displacement response as the optimization objective, the obtained optimal stiffness of TMD k_d^{opt} is 255.4863 kN/m and the optimal damping coefficient

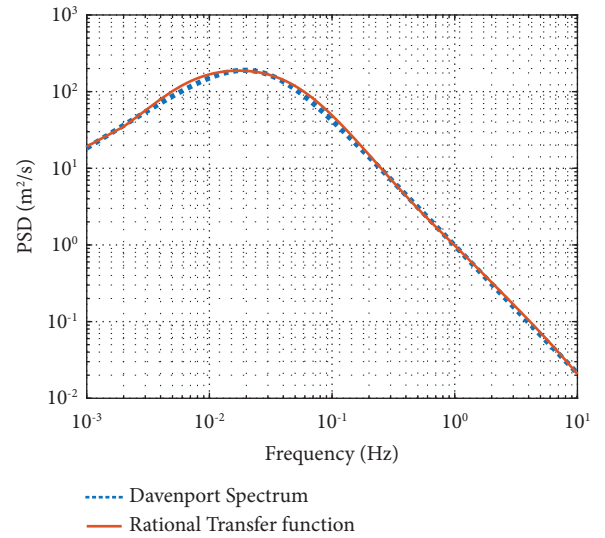

Figure 12: The comparison of Davenport spectrum [47] and the 4-order excitation shaping filter.

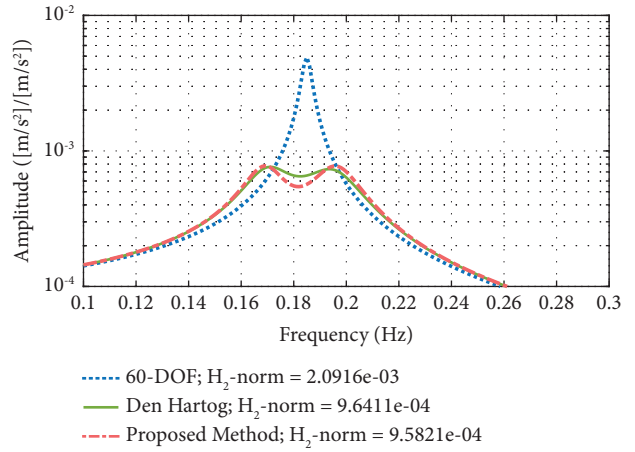

Figure 13: Top-floor displacement frequency response function of the 60-story structure.

c_d^{opt} is 36.3526 kN-s/m. The structural displacement frequency response function is shown in Figure 13 and compared with Den Hartog's design results. As shown in Figure 13, the top-floor displacement of the tuning mode can be reduced effectively. Furthermore, the H_2-norm of the structural displacement is reduced from 20.92×10^{-4} to 9.58×10^{-4}, an improvement over Dan Hartog's result of 9.64×10^{-4}.

The 60-story tall building is modeled as a cantilever beam. Therefore, the top-floor slab of the building will exhibit some rotational behavior due to flexural deformations. However, according to the study of Liu et al. [48], this rotational behavior can be neglected if the structure is within the elastic range, i.e., if the drift ratio of the building is less than 1/200. Moreover, this TMD system is mainly effective in reducing structural vibration for the

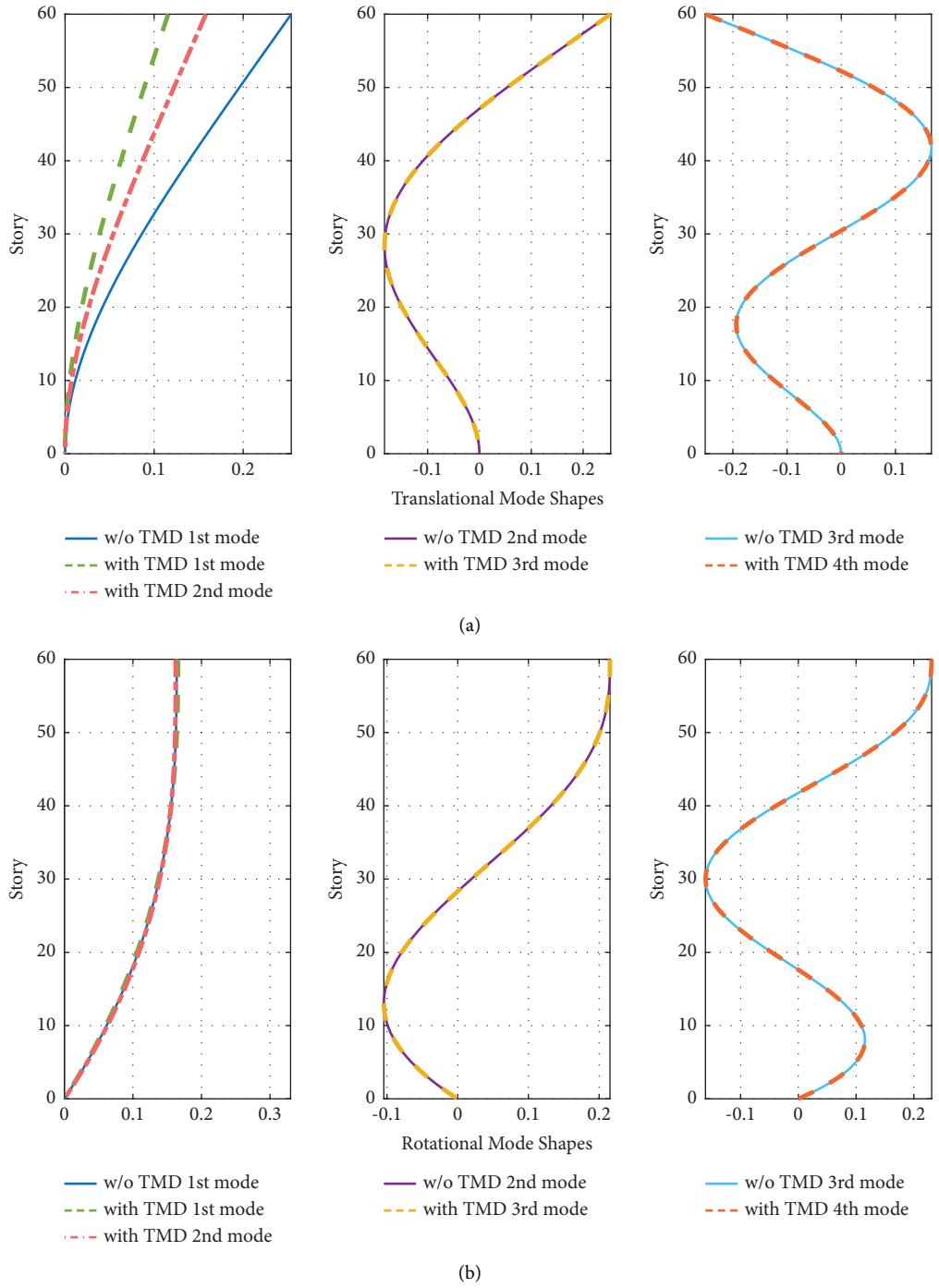

Figure 14: Mode shapes of the DOFs of high-rise building with/without the TMD: (a) translational modes, and (b) rotational modes.

first mode due to the location, such as the top of the building. Figure 14 illustrates the translational and rotational mode shapes of the structural DOFs, where each system mode shape has vector norm of one. In this case, the TMD is designed to tune to the first mode of the structure. Therefore, the first mode of the structure has been separated into two smaller mode shapes, but there are almost no benefits for the other mode shapes. If TMD is desired to reduce vibration in other modes. In that case, the TMD can be optimized by using the higher modal displacement of the structure as the weight matrix for case (D) in Table 1 and placing the TMD on the floor where the most significant building drift of the desired mode occurs. To reduce the vibration of tall buildings across multimodes, Wang et al. [49] proposed a solution that involves using the frequency-independent dampers and negative stiffness devices for this 60-story outrigger building, which can enhance all structural modes simultaneously.

6. Conclusions

By appropriately reconfigurating the parameters in the design of passive TMD, the optimization problem for parameter design can be transformed into an optimization for the nonsparse control gain matrix in static output feedback (also called direct output feedback) of active control. Given this, a general design method is proposed which combines the static output feedback and updates iterative procedure. The followings are concluded for this paper:

(1) The optimal TMD design method proposed in this paper applies to SDOF or MDOF structures, undamped, or damped structures and can be used for structures subjected to random wind loads or earthquake excitations. Depending on the chosen design objective, the corresponding weighting matrix can be casted accordingly based on the selected output matrices. Additionally, the excitation shaping filter can be incorporated in system as required.

(2) According to Parseval's theorem, the optimization result obtained in time domain by the proposed method is equivalent to the optimization of the mean-square response in frequency domain. Therefore, the numerical simulation results demonstrate that the optimal parameters of a SDOF structure equipped with the TMD are consistent with the analytic solution in references. The obtained design parameters can meet the mean square minimization (i.e., H_2-norm minimization) of the objective under random external force.

(3) Since the reconfigured control gain matrix is not a sparse matrix, the static output feedback optimization procedure can be used to solve the optimal gain matrix. The optimal gain matrix for static output feedback is dependent on the initial quadratic condition of the system. To achieve the mean square minimization objective, an analytic initial quadratic condition is presented. This paper also explains how to obtain the analytic initial quadratic condition from state-space external force location matrix.

(4) In the updating iterative procedure, as the required control effort is reduced after the parameter updating, the gain matrix can thus converge to 0. When the gain matrix approaches 0, the design parameters have been updated to the optimal one. This means that even if the active control force is attempted to apply in this situation, a better objective cannot be obtained so the zero gain matrix is given by static output feedback.

(5) The regulator weight R applied for static output feedback is only related to the convergence speed in the iterative procedure but not influence optimal design parameters of TMD after updating. This is because the role of the regulator R in static output feedback is diminished when the gain matrix approaches 0. As long as the regulator weight R is appropriately selected and the simultaneous solution of static output feedback is available, the regulator weight R is not required to be changed in the iterative procedure.

(6) The optimal design parameters for TMDs that minimize the velocity and absolute acceleration of the SDOF structures under random earthquake force are presented for engineers' reference. Examples of designing TMDs for a 5-story MDOF structure subjected to earthquake and a 60-story MDOF structure subjected to wind loads, both considering excitation shaping filter, are also demonstrated in this paper.

Appendix

A. Derivation of Constrained Objective Function

To minimize the following objective function:

$$J = \int_0^\infty \left[\mathbf{z}^T(t)\mathbf{Q}\mathbf{z}(t) + 2\mathbf{z}^T(t)\mathbf{N}u(t) + u^T(t)\overline{R}u(t)\right]\mathrm{d}t, \tag{A.1}$$

when subject to the system dynamics

$$\begin{aligned} \dot{\mathbf{z}}(t) &= \mathbf{A}\mathbf{z}(t) + \mathbf{B}u(t), \\ u(t) &= \mathbf{G}\mathbf{V}\mathbf{z}(t), \\ \mathbf{z}(t) &= e^{(\mathbf{A}+\mathbf{B}\mathbf{G}\mathbf{V})t}\mathbf{z}(0), \end{aligned} \tag{A.2}$$

where $\mathbf{z}(t)$ is the state vector of the system; $u(t)$ is the output feedback control force; $\mathbf{Q}$, $\mathbf{N}$ and $\overline{R}$ are the weightings; $\mathbf{z}(0)$ is the initial condition. Equation (A.2) is substituted in equation (A.1) to obtain

$$J = \mathbf{z}(0)^T\left[\int_0^\infty e^{(\mathbf{A}+\mathbf{B}\mathbf{G}\mathbf{V})^T t}\left(\mathbf{Q} + 2\mathbf{N}\mathbf{G}\mathbf{V} + \mathbf{V}^T\mathbf{G}^T\overline{R}\mathbf{G}\mathbf{V}\right)e^{(\mathbf{A}+\mathbf{B}\mathbf{G}\mathbf{V})t}dt\right]\mathbf{z}(0). \tag{A.3}$$

Usually, a constant positive semidefinite matrix $\mathbf{H}$ can be found to ensure system stability, such that the system response approaches 0 as time approaches infinity, i.e., $\lim_{t\longrightarrow\infty}\mathbf{z}^T(t)\mathbf{H}\mathbf{z}(t) = 0$. The objective function optimization problem of equation (A.3) can be transformed into an initial value problem as follows:

$$J = \mathbf{z}(0)^T\mathbf{H}\mathbf{z}(0) = \mathrm{tr}\{\mathbf{H}\mathbf{Z}_0\}, \tag{A.4}$$

where tr{.} is the trace operation of a matrix. $\mathbf{Z}_0 = \mathbf{z}(0)\,\mathbf{z}(0)^T$ can be treated as a quadratic initial condition matrix. The calculation of constant positive semidefinite symmetric matrix $\mathbf{H}$ must satisfy the state equation and its propagation solution of equation (A.2). Therefore, the Lagrange

multiplier $\mathbf{L}$ is used to substitute the constraint condition. The constrained objective function $\overline{J}'$ is derived as

$$\overline{J}' = \mathrm{tr}\{\mathbf{H}\mathbf{Z}_0 + \mathbf{L}[(\mathbf{A}+\mathbf{B}\mathbf{G}\mathbf{V})^T\mathbf{H} + \mathbf{H}(\mathbf{A}+\mathbf{B}\mathbf{G}\mathbf{V}) + (\mathbf{Q} + 2\mathbf{N}\mathbf{G}\mathbf{V} + (\mathbf{V}^T\mathbf{G}^T\overline{R}\mathbf{G}\mathbf{V}))]\}. \quad (A.5)$$

B. Solution of Lyapunov Equation

A Lyapunov equation meets the following form:

$$\mathbf{A}\mathbf{X} + \mathbf{X}\mathbf{A}^T + \mathbf{Q} = \mathbf{0}, \quad (B.1)$$

where $\mathbf{A}$ matrix is stable (the real part of its eigenvalue is smaller than 0) and $\mathbf{Q}$ matrix is a positive definite matrix, then equation (B.1) has the unique positive definite matrix solution $\mathbf{X}$. To solve $\mathbf{X}$, the Kronecker product can be applied to change the abovementioned equation to

$$[\mathbf{I}\otimes\mathbf{A} + \mathbf{A}\otimes\mathbf{I}]\mathrm{vec}(\mathbf{X}) + \mathrm{vec}(\mathbf{Q}) = 0, \quad (B.2)$$

where $\otimes$ is an operation of Kronecker product, and vec (.) means the matrix is arranged by column vectorization. Therefore, vec ($\mathbf{X}$) can be obtained from equation (B.2) by inverse matrix operation. Then, vec ($\mathbf{X}$) is rearranged by matricization of a square matrix $\mathbf{X}$ to complete the computation.

C. Correction of Damping Ratio Formulae

The optimal TMD design formula of structural acceleration mean-square minimization for a SDOF undamped structure under random wind force was proposed by Korenev and Reznikov [13]. The optimal frequency ratio design formula is expressed as follows:

$$R_f^{\mathrm{opt}} = \sqrt{1 - 0.5R_m}. \quad (C.1)$$

The original optimal damping ratio design formula has no real number solution when the mass ratio is large and is corrected as follows:

$$\zeta_d^{\mathrm{opt}} = \sqrt{\frac{R_m(1 - 0.25R_m)}{2(2 - R_m)(1 - R_m + R_m^2)}}. \quad (C.2)$$

Data Availability

Data used to support the findings of this study are available from the corresponding author upon request.

Conflicts of Interest

The authors declare that they have no conflicts of interest.

References

[1] T. T. Soong and G. F. Dargush, *Passive Energy Dissipation Systems in Structural Engineering*, Wiley, New York, NY, USA, 1997.

[2] A. Li, *Vibration Control for Building Structures: Theory and Applications*, Springer Nature, Berlin, Germany, 2020.

[3] I. Takewaki and H. Akehashi, "Comprehensive review of optimal and smart design of nonlinear building structures with and without passive dampers subjected to earthquake loading," *Frontiers in Built Environment*, vol. 7, Article ID 631114, 2021.

[4] I. Takewaki, *Building Control with Passive Dampers: Optimal Performance-Based Design for Earthquakes*, Wiley, New York, NY, USA, 2009.

[5] H. Frahm, "Device for damping vibration of bodies," United States Patent, Alexandria, VA, USA, 989958, 1911.

[6] J. J. Connor, *Introduction to Structural Motion Control*, Prentice Hall, Hoboken, NJ, USA, 2007.

[7] M. Gutierrez Soto and H. Adeli, "Tuned mass dampers," *Archives of Computational Methods in Engineering*, vol. 20, no. 4, pp. 419–431, 2013.

[8] L. Wang, W. Shi, X. Li, Q. Zhang, and Y. Zhou, "An adaptive-passive retuning device for a pendulum tuned mass damper considering mass uncertainty and optimum frequency," *Structural Control and Health Monitoring*, vol. 26, no. 7, Article ID e2377, 2019.

[9] M. Wang, S. Nagarajaiah, and L. Chen, "Adaptive passive negative stiffness and damping for retrofit of existing tall buildings with tuned mass damper: tmd-nsd," *Journal of Structural Engineering*, vol. 148, no. 11, Article ID 04022180, 2022.

[10] J. P. Den Hartog, *Mechanical Vibrations*, McGraw-Hill, New York, NY, USA, 1956.

[11] H. C. Tsai and G. C. Lin, "Optimum tuned-mass dampers for minimizing steady-state response of support-excited and damped systems," *Earthquake Engineering and Structural Dynamics*, vol. 22, no. 11, pp. 957–973, 1993.

[12] G. B. Warburton, "Optimum absorber parameters for various combinations of response and excitation parameters," *Earthquake Engineering & Structural Dynamics*, vol. 10, no. 3, pp. 381–401, 1982.

[13] B. G. Korenev and L. M. Reznikov, *Dynamic Vibration Absorbers: Theory and Technical Applications*, Wiley, New York, NY, USA, 1993.

[14] S. V. Bakre and R. S. Jangid, "Optimum parameters of tuned mass damper for damped main system," *Structural Control and Health Monitoring*, vol. 14, no. 3, pp. 448–470, 2007.

[15] G. C. Marano and R. Greco, "Optimization criteria for tuned mass dampers for structural vibration control under stochastic excitation," *Journal of Vibration and Control*, vol. 17, no. 5, pp. 679–688, 2010.

[16] O. F. Tigli, "Optimum vibration absorber (tuned mass damper) design for linear damped systems subjected to random loads," *Journal of Sound and Vibration*, vol. 331, no. 13, pp. 3035–3049, 2012.

[17] Y. H. Chen and Y. H. Huang, "Timoshenko beam with tuned mass dampers and its design curves," *Journal of Sound and Vibration*, vol. 278, no. 4-5, pp. 873–888, 2004.
[18] N. Hoang, Y. Fujino, and P. Warnitchai, "Optimal tuned mass damper for seismic applications and practical design formulas," *Engineering Structures*, vol. 30, no. 3, pp. 707–715, 2008.
[19] S. J. Jang, M. J. Brennan, E. Rustighi, and H. J. Jung, "A simple method for choosing the parameters of a two degree-of-freedom tuned vibration absorber," *Journal of Sound and Vibration*, vol. 331, no. 21, pp. 4658–4667, 2012.
[20] T. T. Soong and G. D. Manolis, "Active structures," *Journal of Structural Engineering*, vol. 113, no. 11, pp. 2290–2302, 1987.
[21] L. L. Chung, A. M. Reinhorn, and T. T. Soong, "Experiments on active control of seismic structures," *Journal of Engineering Mechanics*, vol. 114, no. 2, pp. 241–256, 1988.
[22] B. F. Spencer and M. K. Sain, "Control buildings: a new Frontier in feedback," *IEEE Control Systems Magazine*, vol. 17, pp. 19–35, 1997.
[23] J. C. Doyle, K. Glover, P. P. Khargonekar, and B. A. Francis, "State-space solutions to standard H_2 and H_∞ control problem," *IEEE Transactions on Automatic Control*, vol. 34, no. 8, pp. 831–847, 1989.
[24] B. F. Spencer, J. Suhardjo, and M. K. Sain, "Frequency domain optimal control strategies for aseismic protection," *Journal of Engineering Mechanics*, vol. 120, no. 1, pp. 135–158, 1994.
[25] S. J. Dyke, B. F. Spencer, P. Quast, D. C. Kaspari, and M. K. Sain, "Implementation of an active mass driver using acceleration feedback control," *Computer-Aided Civil and Infrastructure Engineering*, vol. 11, no. 5, pp. 305–323, 1996.
[26] A. K. Agrawal and J. N. Yang, "Design of passive energy dissipation systems based on LQR control methods," *Journal of Intelligent Material Systems and Structures*, vol. 10, no. 12, pp. 933–944, 1999.
[27] J. N. Yang, S. Lin, J. H. Kim, and A. K. Agrawal, "Optimal design of passive energy dissipation systems based on H_∞ and H_2 performances," *Earthquake Engineering & Structural Dynamics*, vol. 31, no. 4, pp. 921–936, 2002.
[28] L. Zuo, "Optimal control with structure constraints and its application to the design of passive mechanical systems," Master of Science Thesis, Massachusetts Institute of Technology, Massachusetts, MA, USA, 2002.
[29] L. Zuo and S. A. Nayfeh, "Optimization of the individual stiffness and damping parameters in multiple-tuned-mass damper systems," *Journal of Vibration and Acoustics*, vol. 127, no. 1, pp. 77–83, 2005.
[30] L. Zuo and S. A. Nayfeh, "Structured H2 optimization of vehicle suspensions based on multi-wheel models," *Vehicle System Dynamics*, vol. 40, no. 5, pp. 351–371, 2003.
[31] J. Michielsen, I. Lopez Arteaga, and H. Nijmeijer, "LQR-based optimization of multiple tuned resonators for plate sound radiation reduction," *Journal of Sound and Vibration*, vol. 363, pp. 166–180, 2016.
[32] C. M. Chang, S. Shia, and Y. A. Lai, "Seismic design of passive tuned mass damper parameters using active control algorithm," *Journal of Sound and Vibration*, vol. 426, pp. 150–165, 2018.
[33] C. M. Chang, S. Shia, and C. Y. Yang, "Use of active control algorithm for optimal design of base-isolated buildings against earthquakes," *Structural and Multidisciplinary Optimization*, vol. 58, no. 2, pp. 613–626, 2018.
[34] C. Qu, H. N. Li, L. Huo, and T. H. Yi, "Optimum value of negative stiffness and additional damping in civil structures," *Journal of Structural Engineering*, vol. 143, no. 8, Article ID 04017068, 2017.
[35] Z. F. Shao, X. Tang, L. P. Wang, and X. Chen, "Dynamic modeling and wind vibration control of the feed support system in FAST," *Nonlinear Dynamics*, vol. 67, no. 2, pp. 965–985, 2011.
[36] L. L. Chung, C. C. Lin, and S. Y. Chu, "Optimal direct output feedback of structural control," *Journal of Engineering Mechanics*, vol. 119, no. 11, pp. 2157–2173, 1993.
[37] F. L. Lewis, D. L. Varbie, and V. L. Syrmos, *Optimal Control*, Wiley, New York, NY, USA, 2012.
[38] W. S. Levine and M. Athans, "On the determination of the optimal constant output feedback gains for linear multivariable systems," *IEEE Transactions on Automatic Control*, vol. 15, no. 1, pp. 44–48, 1970.
[39] D. D. Moerder and A. J. Calise, "Convergence of a numerical algorithm for calculating optimal output feedback gains," *IEEE Transactions on Automatic Control*, vol. 30, no. 9, pp. 900–903, 1985.
[40] I. Takewaki, *Critical Excitation Methods in Earthquake Engineering*, Wiley, New York, NY, USA, 2007.
[41] H. Akehashi and I. Takewaki, "Bounding of earthquake response via critical double impulse for efficient optimal design of viscous dampers for elastic-plastic moment frames," *Japan Architectural Review*, vol. 5, no. 2, pp. 131–149, 2022.
[42] H. Akehashi and I. Takewaki, "Resilience evaluation of elastic-plastic high-rise buildings under resonant long-duration ground motion," *Japan Architectural Review*, vol. 5, no. 4, pp. 373–385, 2022.
[43] C. C. Lin, J. F. Wang, and J. M. Ueng, "Vibration control identification of seismically excited m.d.o.f structure-PTMD systems," *Journal of Sound and Vibration*, vol. 240, no. 1, pp. 87–115, 2001.
[44] M. C. Constantinou and I. G. Tadjbakhsh, "Optimum characteristics of isolated structures," *Journal of Structural Engineering*, vol. 111, no. 12, pp. 2733–2750, 1985.
[45] C. M. Chang, Z. Wang, B. F. Spencer, and Z. Chen, "Semi-active damped outriggers for seismic protection of high-rise buildings," *Smart Structures and Systems*, vol. 11, no. 5, pp. 435–451, 2013.
[46] M. Wang, S. Nagarajaiah, and F. F. Sun, "A novel crosswind mitigation strategy for tall buildings using negative stiffness damped outrigger system," *Structural Control and Health Monitoring*, vol. 29, p. e2988, 2022.
[47] M. Wang, S. Nagarajaiah, and F. F. Sun, "Dynamic characteristics and responses of damped outrigger tall buildings using negative stiffness," *Journal of Structural Engineering*, vol. 146, no. 12, Article ID 04020273, 2020.
[48] X. Liu, Z. Qu, Y. Huang, and A. Wada, "Effects of geometric nonlinearities on the vibration reduction performance of tuned mass dampers on top of flexible structures," *Advances in Structural Engineering*, vol. 11, Article ID 136943322211495, 2023.
[49] M. Wang, F. F. Sun, Y. Koetaka, L. Chen, S. Nagarajaiah, and X. Du, "Frequency independent damped outrigger systems for multi-mode seismic control of super tall buildings with frequency independent negative stiffness enhancement," *Earthquake Engineering and Structural Dynamics*, vol. 3891, 2023.